J Oceanogr (2014) 70:211–223
DOI 10.1007/s10872-014-0225-9

ORIGINAL ARTICLE

Regeneration of a warm anticyclonic ring by cold water masses within the western subarctic gyre of the North Pacific

Sachihiko Itoh · Ichiro Yasuda · Hiromichi Ueno · Toshio Suga · Shigeho Kakehi

Received: 6 November 2013 / Revised: 20 January 2014 / Accepted: 13 February 2014 / Published online: 5 March 2014
© The Oceanographic Society of Japan and Springer Japan 2014

Abstract Regeneration of a warm anticyclonic ring as a result of interaction with cold water masses was observed within the western subarctic gyre of the North Pacific. Satellite, profiling float, and shipboard observations revealed that a warm-core ring originated from the Kuroshio Extension, propagating northeastwards, entrained cold and fresh water masses from the coastal area of Hokkaido, which are typically recognized within the ring as water that is colder than 2.5 °C. The potential temperature and planetary contribution of potential vorticity of the cold water in the coastal area of Hokkaido were <2 °C and 15×10^{-11} $m^{-1}s^{-1}$, respectively, suggesting that it originated from the Sea of Okhotsk. After the intrusion, the warm core of the ring cooled, freshened, and contracted, while the outer and lower parts became occupied by the cold and fresh water; however, even after the cooling, the positive surface elevation and downward depression of the main pycnocline, typical of an anticyclonic ring, were still evident. The ring continued to propagate northeastwards, with the main part of its structure occupied by the cold water, but changed its direction of travel from northwest to west-southwest 8 months after the cold-water event, and was finally absorbed into another warm-core ring. It is suggested that these anticyclonic rings, which transported and mixed warm and cold water masses, play important roles in the cross-gyre exchange of subtropical and subarctic waters in the North Pacific.

Keywords Anticyclonic ring · Regeneration · Warm core · Cold core · Kuroshio · Sea of Okhotsk · Cross-gyre exchange · Profiling float

S. Itoh (✉) · I. Yasuda
Atmosphere and Ocean Research Institute, The University of Tokyo, 5-1-5 Kashiwanoha, Kashiwa, Chiba 277-8564, Japan
e-mail: itohsach@aori.u-tokyo.ac.jp

H. Ueno
Faculty of Fisheries Science, Hokkaido University, Sapporo, Japan

T. Suga
Department of Geophysics, Graduate School of Science, Tohoku University, Sendai, Japan

T. Suga
Japan Agency for Marine-Earth Science and Technology, Yokosuka, Japan

S. Kakehi
Tohoku National Fisheries Research Institute, Fisheries Research Agency, Shiogama, Japan

1 Introduction

Western boundary currents of subtropical gyres such as the Kuroshio current and the Gulf Stream frequently pinch off intense anticyclonic rings containing a warm-water core (warm-core rings) to their poleward side (Kawai 1972; Olson et al. 1992; Richardson 1983). Warm-core rings interact with each other, and also with the current of their origin, sometimes absorbing water masses (Cresswell 1982; Joyce et al. 1984; Yasuda et al. 1992). This supply of warm water renews the warm-core, and contributes to the long-term persistence of the rings.

Intense mesoscale anticyclonic rings are known to have long lifetimes, often exceeding 1 year. These rings disappear when they are absorbed by other currents or eddies, or mix with adjacent water masses. Almost all Gulf Stream warm-core rings are re-absorbed into the Gulf Stream (Brown et al. 1986; Evans et al. 1985), while Agulhas rings generally decay in the South Atlantic (Gordon 1985;

Lutjeharms 1988). However, the absorption of the Kuroshio warm-core rings into the western North Pacific is not fully understood.

The Kuroshio warm-core rings are generally observed east of Japan in a transition region between the Kuroshio and the Oyashio currents, together with patches and intrusions of various water masses originating from the Kuroshio Extension (subtropical), the Oyashio current (subarctic), and the Tsugaru Warm Current (Sea of Japan) (Yasuda 2003). Under the influence of the planetary β-effect, the rings in the offshore area of the transition region (typically east of 146°E) propagate westwards until they enter the area near the western boundary, where the Japan Trench runs approximately north–south (Itoh and Yasuda 2010a; Mizuno and White 1983). The rings in this western boundary area interact intensively with the Kuroshio Extension, or other rings propagating from the east (Yasuda et al. 1992). While many of the rings that appear in this western boundary area degrade locally through the absorption into other rings or the Kuroshio Extension, some propagate northwards along the Japan Trench and the Kuril–Kamchatka Trench to enter the subarctic gyre (Itoh and Yasuda 2010a; Kitano 1975; Yasuda et al. 1992).

What remains unclear is the fate of these rings that propagate away from the subtropical gyre. According to subsurface temperature maps compiled from hydrographic observations, approximately half of the Kuroshio warm-core rings detected in the maps (typically west of 146°E) are absorbed into the Kuroshio Extension or the Tsugaru Warm Current, but the process by which the other rings disappear could not be determined: they were lost from the maps, but whether they decayed out or rapidly coalesced with other rings or currents could not be determined (Tomosada 1986).

Using satellite altimetry data, Yasuda et al. (2000) found that a Kuroshio warm-core ring travelled to a point south of the Bussol' Strait near the Kuril Islands in June 1995. As later hydrographic observations (July–August 1995) showed that it included small cold-water patches (<2 °C) in its core, they suggested that the ring was supplied with water from the Sea of Okhotsk. In December, the ring began to decay and move southwestwards, and was not observed in the area near the Bussol' Strait until February 1996; however, whether it had decayed locally or moved away from the area, again remained unconfirmed.

On becoming detached from the Kuroshio Extension, the warm-core rings were observed to lose their heat through atmospheric cooling and horizontal/vertical mixing especially during winter. The temperature of the upper core decreased by about 5–6 °C from the 14–15 °C typical of the Kuroshio Extension during the first winter (Tomosada 1986; Yasuda et al. 1992), and by 3–4 °C during the second winter. Itoh et al. (2011a) also reported that the winter temperature drop of a matured ring that had already been cooled was substantially smaller in range than that of fresh rings, which had been observed to change by from 5.5 to 5.0 °C. Although these processes weaken the signal obtained from the warm core of the rings, it remains unclear whether they are primarily responsible for extinguishing the Kuroshio warm-core rings. While Yasuda et al. (2000) found that a Kuroshio warm-core ring near the Bussol' Strait entrained cold-water patches into its core, Itoh and Yasuda (2010b) revealed that Kuroshio warm-core rings located further south also have a cold water mass below the warm core at a potential density range around 26.7 σ_θ, and they suggested that rings with a warm and saline core are coupled with anticyclonic eddies with a cold freshwater core originating from the Sea of Okhotsk.

Itoh et al. (2011a) investigated variations in temperature and salinity profiles of a single ring propagating northeastward within the subarctic gyre using year-long continuous observations from two profiling floats. Although the presence of the cold and fresh lower core was well defined in this ring, the floats were detrained from the ring before the water mass characteristics were completely modified or the potential energy was all lost. As the timescale of viscous decay was estimated to be several years for this ring, it is unlikely that prominent rings decay out within a timescale of months, at least when they are isolated.

Therefore, in the present study, temperature and salinity profile data obtained within and across such a ring were analyzed to examine the fate of the mature Kuroshio warm-core rings. We searched for the target ring in areas away from the Kuroshio Extension, and subsequently deployed one profiling float into a ring off Kushiro in August 2009 (hereafter referred to as Ring K09) from the R/V *Hakuho-Maru*, while two additional profiling floats deployed by the Japan Meteorological Agency (JMA) also made observations of this ring. In addition, seasonal hydrographic observations were conducted by the JMA and Fisheries Research Agency of Japan in this area from the coast to the offshore areas.

The remainder of this paper is organized as follows. The data from the profiling floats, shipboard observations, and satellite are described in Sect. 2. The variations in the structure and core water properties are described in Sect. 3, with a particular focus on a cold-water intrusion event in early 2010. Finally, the behavior and fate of anticyclonic rings originating from the Kuroshio Extension, and their roles in heat/material transport and the formation of water masses, are discussed in Sect. 4.

Table 1 Metadata from profiling floats A, B, and C

	WMO-ID	Profile		Parking depth (dbar)	Profile date in Ring K09		
		Cycle (days)	Depth (dbar)		First	Last	Duration (days)
A	2900946	5	2,010	1,000	26 Jan 2009	16 Jan 2010	355
B	2900966	5	500	500	14 Aug 2009	27 Dec 2010	501
C	2900987	5	2,010	1,000	07 Jul 2010	05 Oct 2010	91

2 Materials and methods

The three profiling floats A, B, and C, have World Meteorological Organization (WMO) IDs of 2900946, 2900966, and 2900987, respectively (Table 1), and their data were downloaded from the mirror site of the Global Data Assembly Centre maintained by the Japan Argo Delayed-mode Data Base (http://www.jamstec.go.jp/ARGO/argo_web/argo/index_e.html). All three floats had a conductivity–temperature–depth (CTD; SBE41, SeaBird Electronics) sensor, and recorded pressure, temperature, and salinity. Floats A and C were parked at 1,000 dbar, and observed temperature and salinity profiles from the surface (ca. 5 dbar) to 2,010 dbar, while float B was parked at 500 dbar, and obtained profiles from the surface (ca. 5 dbar) down to 500 dbar. Although measured pressure levels differed slightly from profile to profile, the data were interpolated to standard pressure levels every 5 dbar. For floats A and C, dynamic height anomalies (DHAs) at 15 dbar with a reference level of 1,985 dbar (maximum available range for all profiles) were calculated, integrating specific volume anomalies over this range with a reference temperature and salinity of 0 °C and 35 psu, respectively.

In addition to the profiling float data, CTD (SBE9plus, SeaBird Electronics) and expendable CTD (XCTD; Tsurumi-Seiki) data obtained during five research cruises (KH0910, KH1001, WK1003, KS1003, and WK1005) across or around Ring K09 were also analyzed (Table 2). Among the five cruises, KH0910 in October–November 2009, WK1003 in March 2010, and KS1003 in May 2010 captured the center of the ring. The CTD observations were typically conducted at depths below 2,000 dbar, or to the bottom in shallow waters, whereas XCTD data were available above 1,000 dbar. As for the data from floats A and C, DHAs were calculated for the CTD data using the same pressure range (15–1,985 dbar). For WK1003, horizontal velocity data were also measured by a shipboard acoustic Doppler current profiler (ADCP); processed data were available down to approximately 1,000 m, with an interval of 32 m. The data from KH1001 and WK1005 obtained from around the ring were also used to determine the horizontal distribution of water masses.

We used weekly absolute sea surface height (SSH) and SSH anomaly data, as produced by the Segment Sol multimissions d'ALTimétrie, d'Orbitographie et de localisation précise/Data Unification and Altimeter Combination System (Ssalto/Duacs) and distributed by the archiving, validation, and interpretation of satellites oceanographic data (AVISO) project, with support from the Centre National d'Etudes Spatiales (CNES). The satellite sea surface temperature (SST) maps used in the present study were compiled by the New Generation Sea Surface Temperature Development Group of Tohoku University, Japan (Sakaida et al. 2009).

Table 2 Metadata from the shipboard observations

Cruise	Ship	Institute	Data used		
			Line	Obs.	Period
KH0910	*Kofu-maru*	JMA[a]	KS	CTD[c]	20 Oct–2 Nov 2009
KH1001	*Kofu-maru*	JMA	KS	CTD	11–13 Feb 2010
WK1003	*Wakataka-maru*	TNFRI[b]	A	CTD, XCTD[d], ADCP[e]	4–7 Mar 2010
KS1003	*Keifu-maru*	JMA	KS	CTD	10–11 May 2010
WK1005	*Wakataka-maru*	TNFRI	A	CTD	12–18 May 2010

[a] Japan Meteorological Agency
[b] Tohoku National Fisheries Research Institute
[c] Conductivity–temperature–depth profiler
[d] eXpendable CTD
[e] Shipboard ADCP

From the SSH anomaly η, the Okubo–Weiss parameter (Okubo 1970; Weiss 1991) $W = 4\ g/f\,[(\partial^2\eta/\partial x\partial y)^2 - (\partial^2\eta/\partial x^2)(\partial^2\eta/\partial y^2)]$ was calculated to obtain the position and amplitude of Ring K09, where g and f are the acceleration due to gravity and the Coriolis parameter, respectively. The core area of Ring K09 was specified by pixels in η maps with negative W below the threshold $-2 \times 10^{-12}\ s^{-2}$ (Chelton et al. 2007), where the relative vorticity anomaly $\zeta = g/f\,(\partial^2\eta/\partial x^2 + \partial^2\eta/\partial y^2)$ was found to be negative. The amplitude of the ring was estimated from the minimum ζ and maximum η values. Note that the temporal variation in η includes steric fluctuations caused by seasonal heating/cooling.

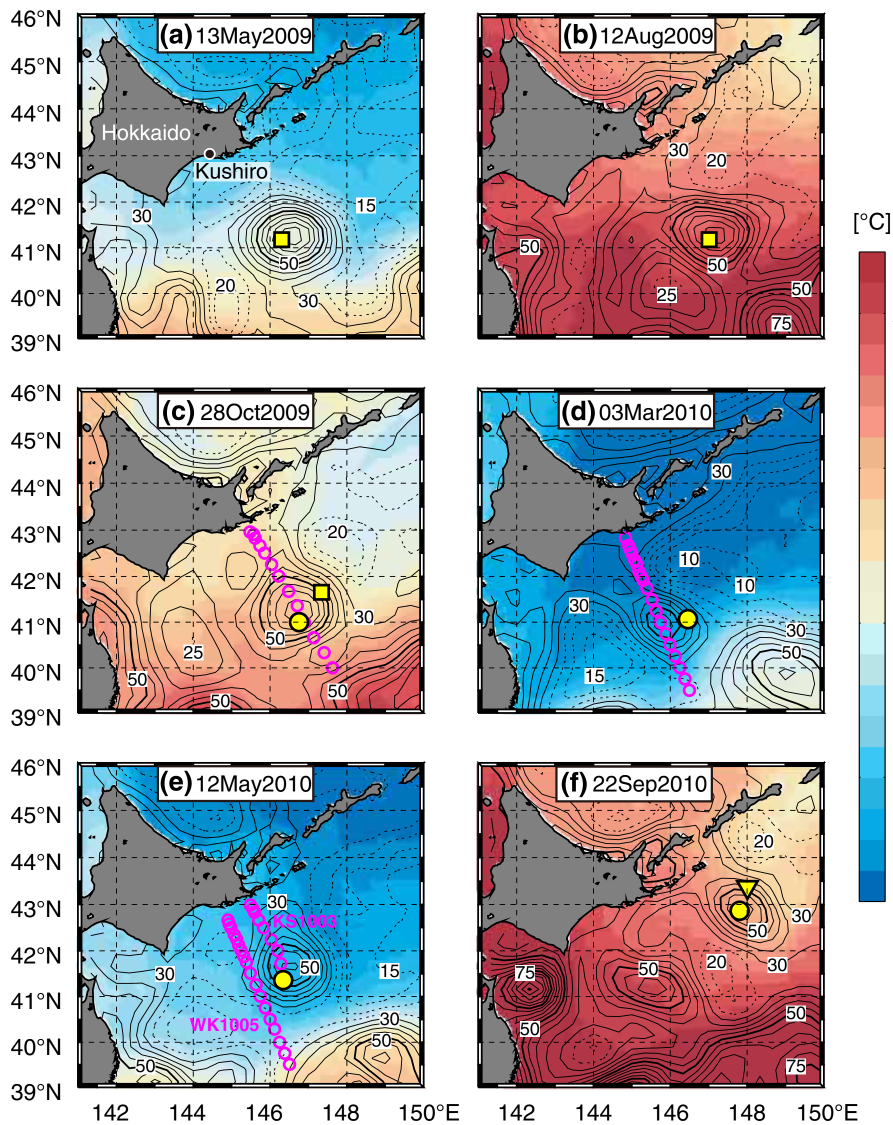

Fig. 1 Time series of sea surface height (*SSH black contours*, contour interval = 5 cm) and temperature (*SST* °C, *color shading*) obtained from the profiling float observations in the study area (northwestern North Pacific), as derived from satellite data. To highlight anticyclonic rings, *dashed contour lines* are used for SSH <25 cm, and *thicker contour lines* for SSH of 50 and 75 cm. *Squares*, *circles*, and *triangles* in and around the closed contours (corresponding to Ring K09) indicate the most recent positions of floats A, B, and C, respectively, which recorded the temperature and salinity profiles of Ring K09. In (**c**–**e**), shipboard observation stations are indicated by *pink circles*

3 Results

3.1 Ring K09 behavior overview

We first provide an overview of fluctuations in the surface conditions of Ring K09, which were determined mainly from satellite data for the period January 2009 to December 2010, when the profiling float data were also available. Over the course of the 2 years, Ring K09 was detected in SSH maps as closed contours of elevation (Fig. 1). During 2009, the SST field of Ring K09 was observed as either a patch or a crest of warm water (Fig. 1a–c), which is as expected for a typical warm-core ring. However, this feature altered in early 2010 (Fig. 1d–f). After March 2010, the cold water was observed in Ring K09. While seasonal cooling in the surface water was widely observed from October 2009 (Fig. 1c) to March 2010 (Fig. 1d), the temperature field around the ring changed from crest to trough: the cold anomaly was more clearly seen in May 2010 (Fig. 1e). Despite this change in the SST field, SSH was still relatively high.

Variations in the position and surface amplitude of Ring K09 were tracked in SSH anomaly maps using the method proposed by Isern-Fontanet et al. (2003) and Chelton et al. (2007). Ring K09 gradually propagated northeastwards over the 2-year period (Fig. 2), as is generally the case for warm-core rings in this region (Itoh and Yasuda 2010a). The mean propagation speed over the 2 years was 0.85 cm s^{-1} toward 41.4° true. Floats A and B generally followed the ring's propagation within its core area (latitudinal and longitudinal ranges of the core area are indicated in Fig. 2a, b as errorbars), whereas float C circulated around the periphery of the core area (suggested by oscillations in Fig. 2a, b). Ring K09 maintained anticyclonic

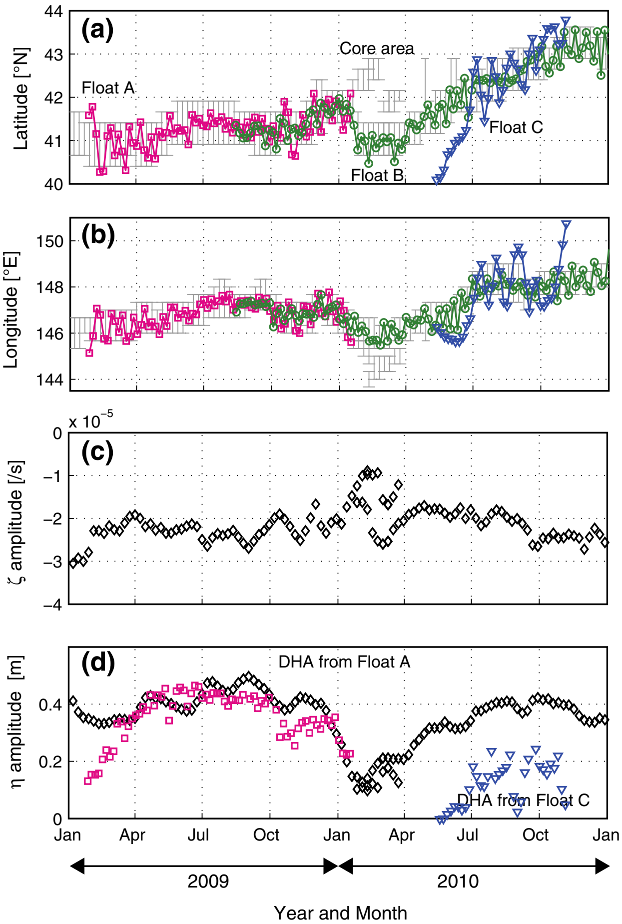

Fig. 2 Time series of float position and ring amplitude. **a** Float latitude (*colored symbols* with *lines*) and latitudinal extent (*gray bars*) of the core area (that with negative *W* value; Itoh and Yasuda 2010a) of Ring K09 as estimated from the SSH anomaly. **b** As (**a**), but for longitude. **c** Amplitude (minimum) in relative vorticity anomaly ζ and **d** amplitude (maximum) in surface elevation η, within the core area of Ring K09. In (**d**), dynamic height anomalies (DHA) calculated from the profiles of floats A and C are also shown with a constant of 1.6 m subtracted to match the level of the SSH anomaly

features throughout this period, as indicated by its negative relative vorticity, but positive surface elevation and DHA. Because float C was located at the periphery of the core area, the calculated DHAs are at a relatively lower level than those calculated from float A.

The core water of Ring K09 was disturbed for a short period. From January to April 2010, Ring K09 was deformed and the main core shifted southwestward in the short term with float B. Eddy amplitudes indicated by the anomalies of relative vorticity and surface elevation were also weakened during this period. Considering the change of the water from warm to cold as seen in Fig. 1, we assume that there was a cold-water intrusion event and/or mixing during this period (hereinafter referred to as the cold-water event). Although Ring K09 apparently changed as an anticyclonic eddy covered with a cold water, detailed descriptions of the evolution and modification of the ring are necessary if we are to fully understand this event. In the following three sections, we present continuous time series of the core water profiles (Sect. 3.2), and also the ring structure before and in the middle of (Sect. 3.3), as well as after (Sect. 3.4), the cold-water event.

3.2 Time series of core water profiles

Temperature and salinity profiles from the floats are consistent with the description based on the SSH field (Fig. 3). From late April to early December 2009, floats A and B observed a homogeneous layer with a temperature of 7–8 °C and salinity of 34.0–34.1 psu below the seasonal pycnocline at approximately 100–400 dbar. The potential density of this layer was 26.5–26.6 σ_θ (kg m^{-3}).

After late December 2009, winter mixing penetrated the seasonal pycnocline to form a deep mixed layer with temperature, salinity, and potential density of 5–7 °C (vertically homogeneous, but decreasing with time), 33.9–34.0 psu, and 26.6–26.7 σ_θ, respectively (Fig. 3c, d). The layer reached almost 400 dbar in late February. These variations until February were typical of the decay of warm-core rings under winter atmospheric cooling and consequent convection and mixing (e.g., Yasuda et al. 1992).

However, at the beginning of March, it began to be eroded by cold freshwater from both above and below. In April, the mixed layer became shallower than 100 dbar, and the core of Ring K09, as originally characterized by the warm and saline water, was barely recognizable with a thickness <100 dbar. Instead, cold water, typically below 2.5 °C, appeared below this anomaly at 26.7–26.9 σ_θ with a thickness of 200–300 dbar. It is noted that the cooling of the core water with a shoaling mixed layer cannot be explained by the normal seasonal cooling from the atmosphere.

The temporal evolution of the core waters of Ring K09 after this drastic modification was observed by floats B and C, which were trapped near the center and the periphery, respectively (Fig. 3c–f). Although DHAs were not calculated for the data obtained by float B because the shallow profiles (down to 500 dbar), depths of 26.8–26.9 σ_θ were deeper for float B (depth of 26.9 σ_θ was approximately 500 dbar) than for float C (depth of 26.9 σ_θ approximately ranges 300–400 dbar), which confirms that float B was kept within the ring. The temperature and salinity of the warm core gradually decreased, while the lower and outer cores (as observed by floats B and C, respectively) were occasionally thickened and cooled, typically from August to October 2010.

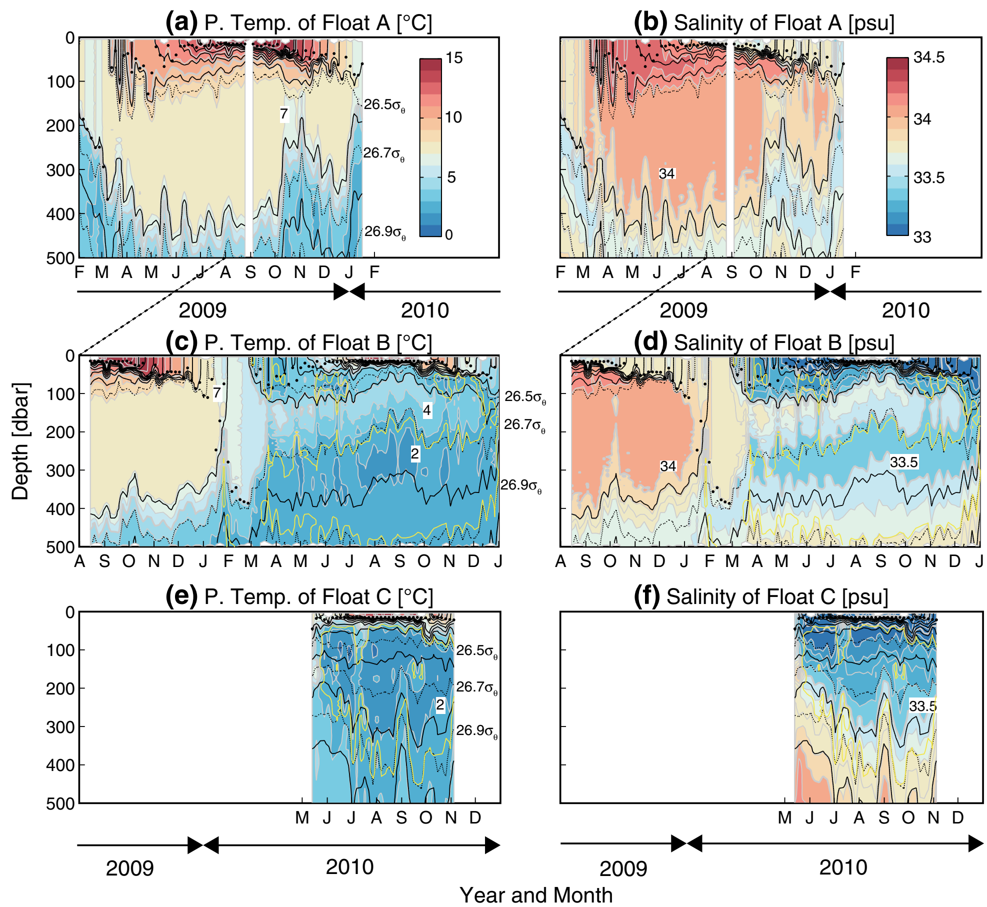

Fig. 3 Evolution of potential temperature and salinity profiles as observed by floats A, B, and C. Temperature (**a**, **c**, and **e**: contour interval = 1 °C) and salinity (**b**, **d**, and **f**: contour interval = 1 psu) are shown by *color shading* with *gray contours*, and *black dots* denote mixed layer depth (*all panels*). *Black solid* (*dotted*) *contour lines* denote potential density with contour interval of 0.2 σ_θ (contour lines of 26.5, 26.7, and 26.9 σ_θ), and *yellow lines* indicate 2.5 °C isotherms

3.3 Ring structure before and during the cold-water event

The hydrographic observations in October–November 2009, before the cold-water event, show that the warm and saline homogeneous water at 100–400 dbar (7–8 °C, 34.0–34.1 psu) formed the core of the ring around 41–42°N, in contrast to the water of <4 °C and <33.7 psu outside this region (Fig. 4a, b). Although the homogeneous warm and saline core water was confined above 400 dbar, a low potential-density anomaly near the center of the ring (i.e., a depression in the isopycnal surface) was observed down to 2,000 dbar.

In early March 2010, a cold freshwater region developed on the northwestern side of the warm core of Ring K09 (Fig. 5). The potential temperature and salinity of the cold water mass had minimum values of around 0.1 °C and 32.4 psu, respectively, in the upper 100 dbar between 41° and 41°25′N. In addition, DHA was elevated above the coupling warm and cold cores. Satellite SSH anomalies interpolated at the CTD did not coincide with DHAs near the center of the ring where a rapid interaction was likely in progress, whereas SSH anomalies over XCTD stations where DHAs were not calculated because of the shallower (1000 dbar) profiles than CTD indicate that the ring kept its structure as an anticyclonic eddy in a longer time scale. The cold fresh anomalies extended deeper than 400 dbar below the warm core, as indicated by the 2.5 °C (yellow) isotherms; however, they did not reach the southeastern side of the ring at this time.

In the southern half of the ring, the core with relatively warm and saline water was still observed. As indicated in Fig. 3c, d, potential temperature, salinity, and potential density of the core were changed by the winter cooling to 5–6 °C, 33.6–33.8 psu, and 26.5–26.7 σ_θ, respectively, before this shipboard observation in March 2010, whereas there was a substantial decrease in the core volume from the autumn of 2009, which was not explained by the winter cooling.

As the potential density of the intruding cold (<2.5 °C) water ranged approximately from 26.6 to 26.8 σ_θ, mean potential temperature and planetary contribution of potential vorticity defined as $Q = gf\partial\sigma_\theta/\partial p$ were calculated for layers of 26.6–26.7 and 26.7–26.8 σ_θ using the shipboard (KH1001 and WK1003) and float (B) data during the ring transect of KH1001 (11–13 February) and WK1003 (4–7 March) cruises (Figs 6, 7). The layer at 26.6–26.7 σ_θ also corresponded to the lower part of the remaining warm core.

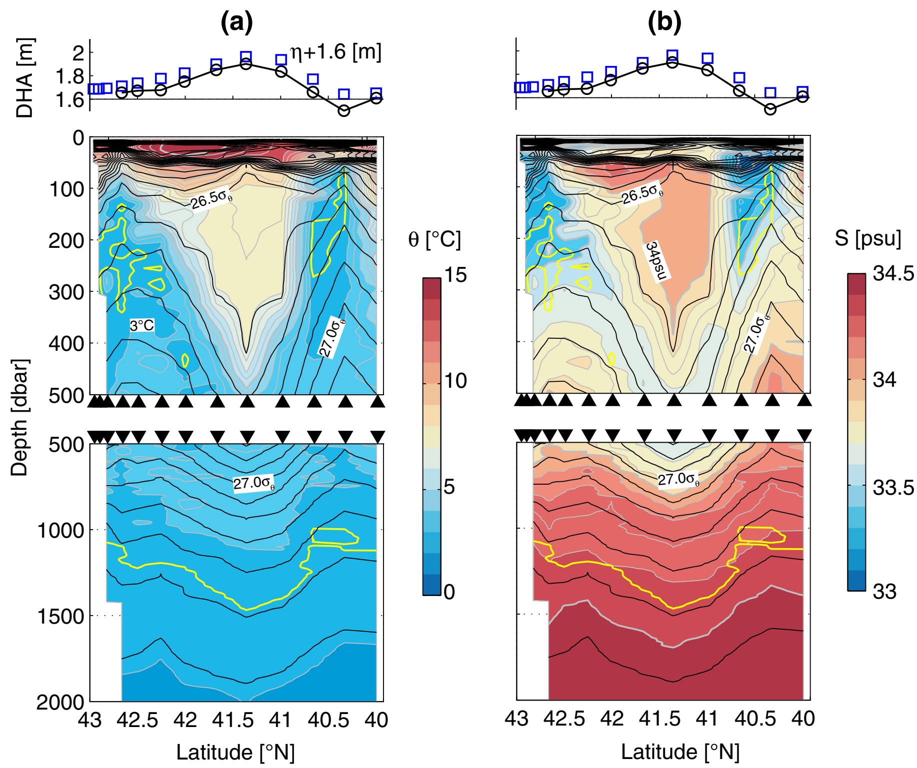

Fig. 4 Structure of Ring K09 during cruise KH0910 in October–November 2009. Potential temperature (θ) and salinity (S) cross-sections are shown in (**a**) and (**b**), respectively, and the dynamic height anomaly (*DHA black lines* and *circles*) and satellite SSH anomaly (η: *blue squares*) are shown at the top of these cross-sections. To focus on upper layer structure, cross-sections are divided into two ranges of 0–500 dbar (*middle panels*) and 500–2,000 dbar (*bottom panels*). *Color shading* with *gray contour lines* shows θ or S, *thin black lines* denote potential density, and *yellow lines* indicate 2.5 °C isotherms. *Black triangles* at 500 dbar denote the positions of the CTD surveys. Contour intervals are 0.5 °C for potential temperature, 1 psu for salinity, and 0.1 σ_θ for potential density

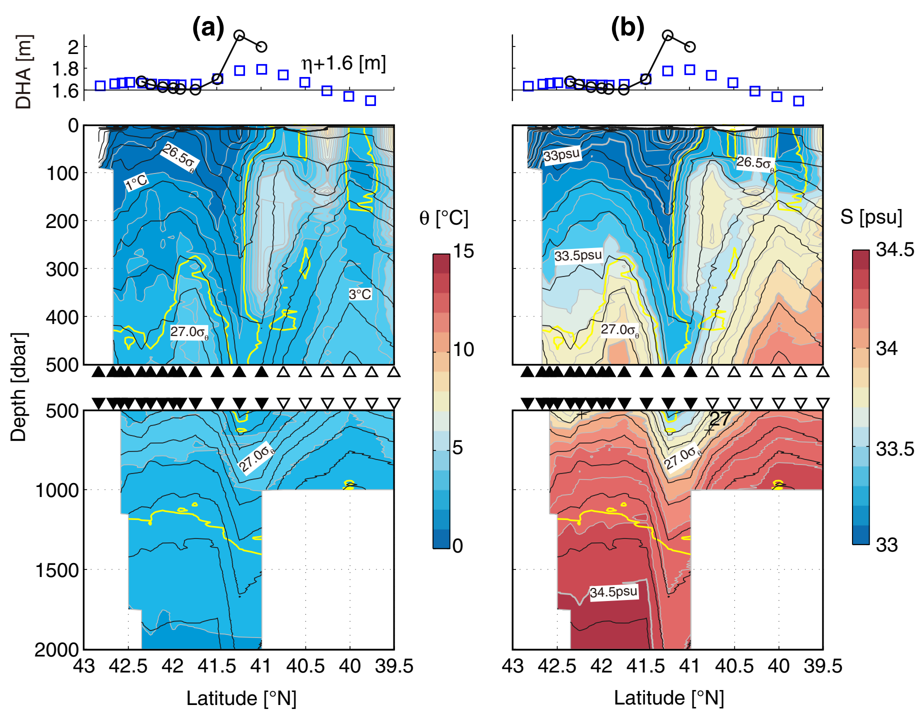

Fig. 5 As for Fig. 4, but during cruise WK1003 in March 2010. The southern half of the ring was observed by XCTD (the positions are indicated by *white triangles*), hence the profiles below 1,000 dbar were not obtained, and DHAs at these stations were not calculated

Although relative vorticity is generally not negligible for mesoscale eddies, the approximate magnitude of the relative vorticity for Ring K09 calculated from the satellite SSH anomalies (Fig. 2d) was 1/5–1/3 ($1.5–3.0 \times 10^{-5}$ s^{-1}) of the planetary vorticity (9.5×10^{-5} s^{-1}) at 41°N.

In February, the layer-mean potential temperature from the east to the north of the ring (north of 40°20′N) was 1.2–2.1 °C at 26.6–26.7 σ_θ (Fig. 6a), and 1.7–2.6 °C at 26.7–26.8 σ_θ (Fig. 6c). A potential temperature lower than 2 °C was mainly recorded in the northwestern area near

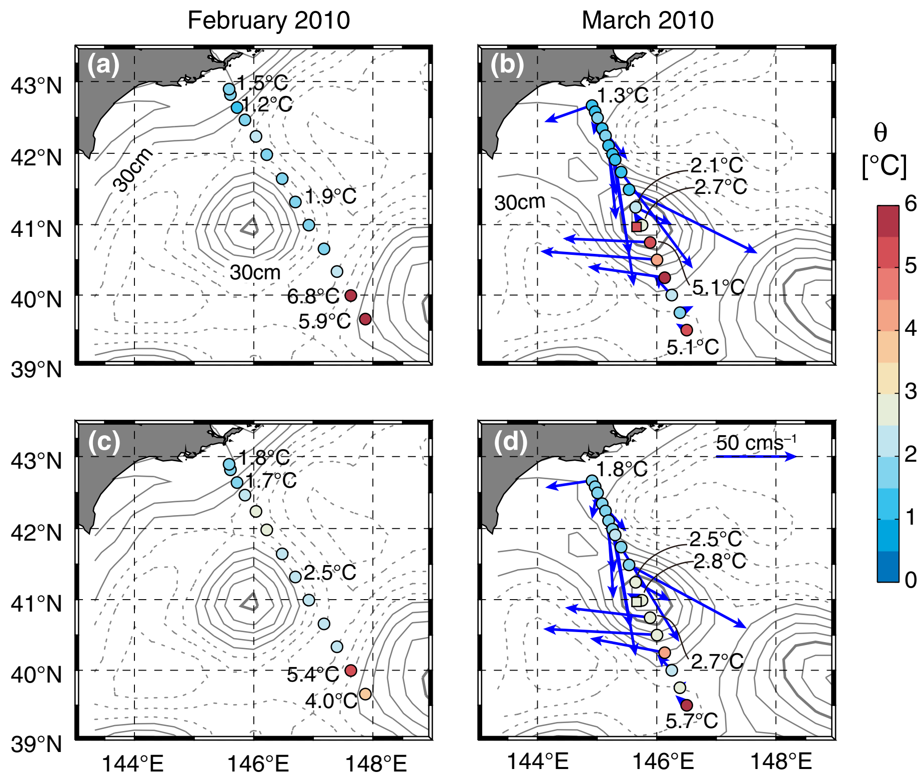

Fig. 6 Distributions of mean potential temperature on isopycnal surfaces. Data were obtained either during 11–13 February 2010 (**a**, **c**) or 4–7 March 2010 (**b**, **d**), and are averaged over either 26.6–26.7 σ_θ (**a**, **b**) or 26.7–26.8 σ_θ (**c**, **d**). Data from shipboard observations and float B are shown with *colored circles* and a *square* (only one profile was available from 7 March), respectively. In (**b**) and (**d**), horizontal velocity vectors obtained from shipboard ADCP are drawn with *magenta arrows*. Background *gray contours* are SSH with same line type as Fig. 1

Hokkaido (Fig. 1a), where SSH was slightly elevated. In March, the area of SSH >30 cm had extended northwestwards, and the cold water was continuously observed from the coastal area of Hokkaido close to the center of the ring (Fig. 6b, d): potential temperature was mainly below 2.5 °C north of 41°30′N at both 26.6–26.7 (1.2–1.7 °C) and 26.7–26.8 (1.6–2.0 °C) σ_θ. Prominent southeastward flows north of 41°15′N suggest that the cold water that was distributed along the coast of Hokkaido in February intruded into the ring in March.

In the southeastern part of the ring, around 40°15′–41°00′N, water warmer than 5 °C was observed at 26.6–26.7 σ_θ (Fig. 6b), as is also seen in the cross-section in Fig. 5. Horizontal velocity essentially followed the azimuthal direction, and intrusion or extrusion was not observed. However, the potential temperature distribution within the southwestern part was more complex and patchy than that to the northeast. Four CTD datasets from WK1003 (circles over 40°15′–41°00′N in Fig. 6b) show spatial heterogeneity, while the difference in potential temperature near the center observed during WK1003 (1500 hours on 6 March, a circle at 40°N), and by float B (0833 hours on 7 March, a square near 40°N), indicate rapid fluctuations in water distribution in this area.

Waters of low Q values, typically <15 × 10^{-11} $m^{-1}s^{-1}$, were observed in the coastal area of Hokkaido, within Ring K09, and along the path connecting these two areas (Fig. 7). These areas essentially correspond to those with relatively high SSH values, except for data from the 26.6–26.7 σ_θ level around the southern periphery of Ring K09 (Fig. 7b). The lowest Q values were calculated near the center of the ring (Fig. 7b). In the low potential temperature range of <2.5 °C, Q generally decreased with decreasing potential temperature at both 26.6–26.7 σ_θ (Fig. 7a, b; $r = 0.57$, $p < 0.01$) and 26.7–26.8 σ_θ (Fig. 7c, d; $r = 0.75$, $p < 0.01$).

3.4 Ring structure and fate after the cold-water event

After the cold-water event, the warm core was observed as a small upper core in the potential density range of 26.6–26.7 σ_θ along the transect during KS1003 cruise in May 2010 (Fig. 8). The potential temperature of the warm core that had not been out-cropped since March 2010 decreased by approximately 0.5 °C from March 2010, which suggests the mixing with the ambient cold water. The waters below (ca. 250–500 dbar around 41°43′–42°N) and adjacent to (ca. 100–350 dbar around 42°14′–42°30′N) the warm core were replaced by cold (1.0–2.5 °C) fresh (33.2–33.7 psu) water. However, the layers at 26.7–26.9 σ_θ below the warm core, and 26.6–26.8 σ_θ beside the warm core, were relatively thick (low potential vorticity) and contributed to the depression of the isopycnal surfaces, typically below 26.8 σ_θ, and resulted in elevation of the dynamic height

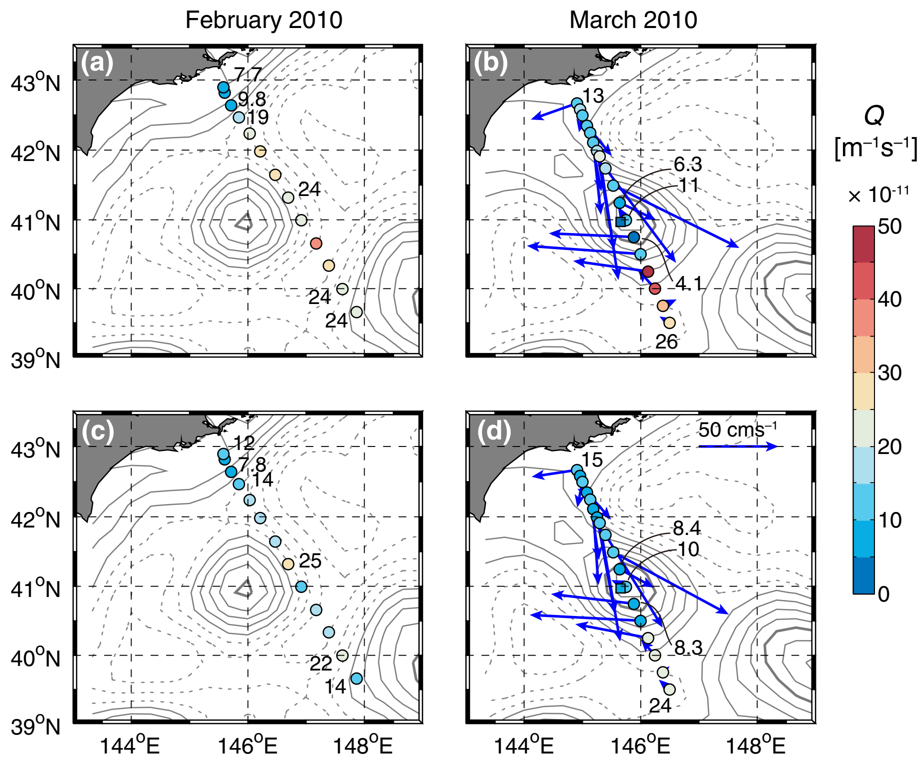

Fig. 7 As for Fig. 6, but for planetary contribution of potential vorticity (Q). Values of Q ($\times 10^{-11}$ m^{-1}s^{-1}) at representative stations are shown within the figure

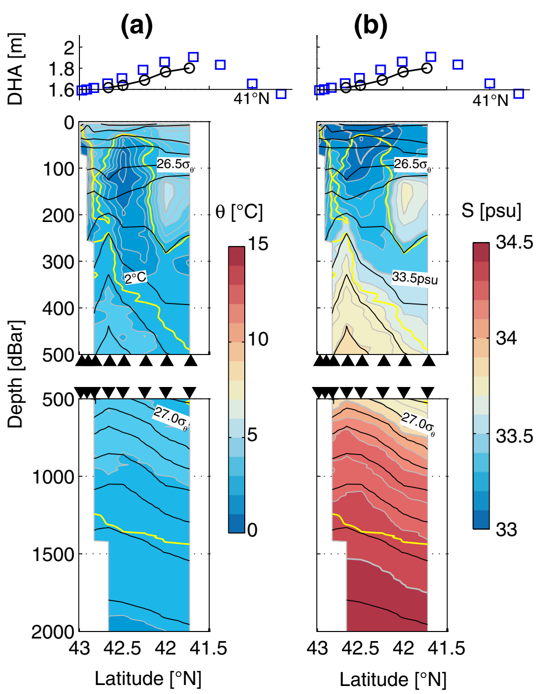

Fig. 8 As for Fig. 4, but during cruise KS1003 in May 2010. SSH anomalies south of 41°45′N were estimated at CTD stations of KH0910 cruise (Fig. 1c)

anomaly. These cold and thick water masses in the 26.7–26.9 σ_θ and 26.6–26.8 σ_θ layers are hereafter referred to as the lower and outer cores, respectively.

Cold water causing the depression of isopycnal surfaces was also observed at the southwestern periphery of the ring along the longer transect during cruise WK1005 in the same month of May 2010 (Fig. 9). Although positive signals of DHA and SSH anomaly were less prominent than the KS1003 transect, distribution of the water with low temperature (typically <2.5 °C) and low salinity down to 300 dbar corresponded to the deepening of isopycnal surfaces and the surface elevations in 41°–41°45′N. The potential temperature, salinity, and potential density profiles at 41°15′N on this southwestern transect was similar to those at 42°30′N northwest of the ring's center (Fig. 8), suggesting the outer core also existed at the southwestern edge of Ring K09. Throughout the southwestern transect, no remnant of the warm core before the cold water event (5–6 °C, 33.6–33.8 psu, and 26.5–26.7 σ_θ) was observed.

The distributions of potential temperature and Q at 26.6–26.7 and 26.7–26.8 σ_θ in May 2010 are shown in Fig. 10. At this time, these layers approximately represent the warm core and the lower core, respectively, while the outer core was distributed over both layers. Unlike in March 2010, the ring was no longer connected to the cold coastal water off Hokkaido. The transect of KS1003 extended up to the center of the ring (at 1814 hours on 11 May) and did not go further south; however, two profiles by float B (at 0841 hours on 11 May and 0836 hours on 16 May, shown by squares) suggest that there was a ring-like band of warm water (4–5 °C) within the warm core

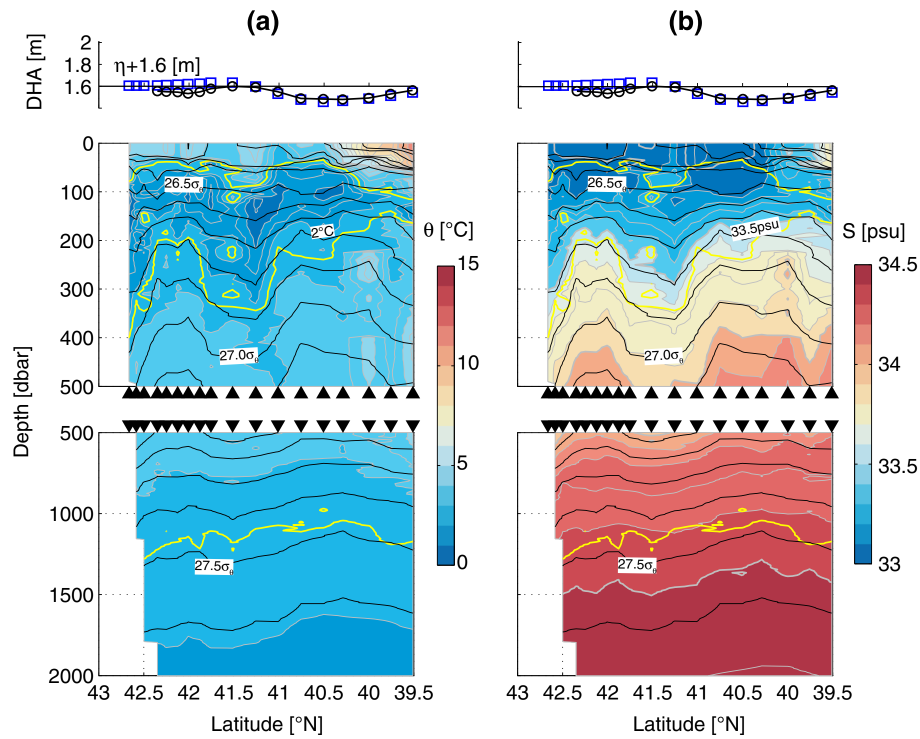

Fig. 9 As for Fig. 4, but during cruise WK1005 in May 2010

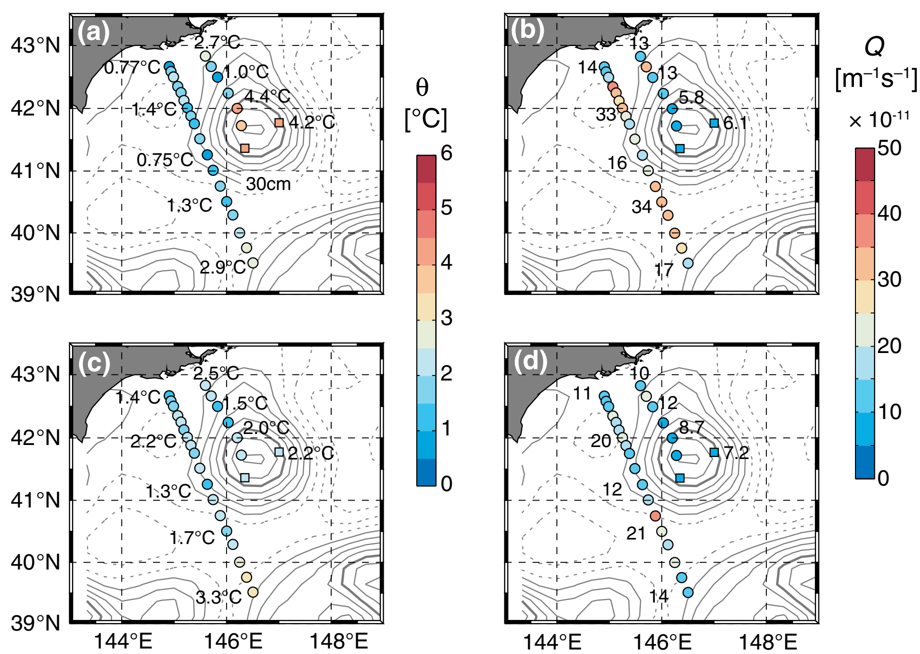

Fig. 10 Distributions of potential temperature θ and planetary contribution of potential vorticity Q in May 2010 (during the ring transect periods of cruises KS1003 and WK1005, 10–18 May): **a** mean θ at 26.6–26.7 σ_θ, **b** Q at 26.6–26.7 σ_θ, **c** mean θ at 26.7–26.8 σ_θ, and **d** Q at 26.7–26.8 σ_θ. Data from shipboard observations and float B are shown with *colored circles* and *squares*, respectively. Background *gray contours* are SSH with same line types as in Fig. 1

(Fig. 10a). Potential temperature and Q at 26.6–26.7 and 26.7–26.8 σ_θ along the southwestern transect were minimum at 41°15′N, 145°38′E which was suggested to be within the outer core.

After May 2010, occasional cold water intrusions to intermediate layers at 26.7–26.9 σ_θ were suggested in profiles from float B (Fig. 3), but Ring K09 was detectable in SSH maps as an anticyclonic ring (Figs 1, 10a, b). Ring K09 continued to propagate northeastwards until November 2010, when the center of the ring was detected at 43°12′N, 148°18′E (Fig. 2). The northeastward propagation almost stopped in late November, and then it gradually propagated west by southwestward (Fig. 11). Although Ring K09 was not observed to merge with other rings (such as that found at 41°30′N, 145°45′E in Fig. 11c), minor interactions with other water masses were indicated by the weekly SSH maps (not shown) and the profile data of float B; however, Ring K09 essentially retained its

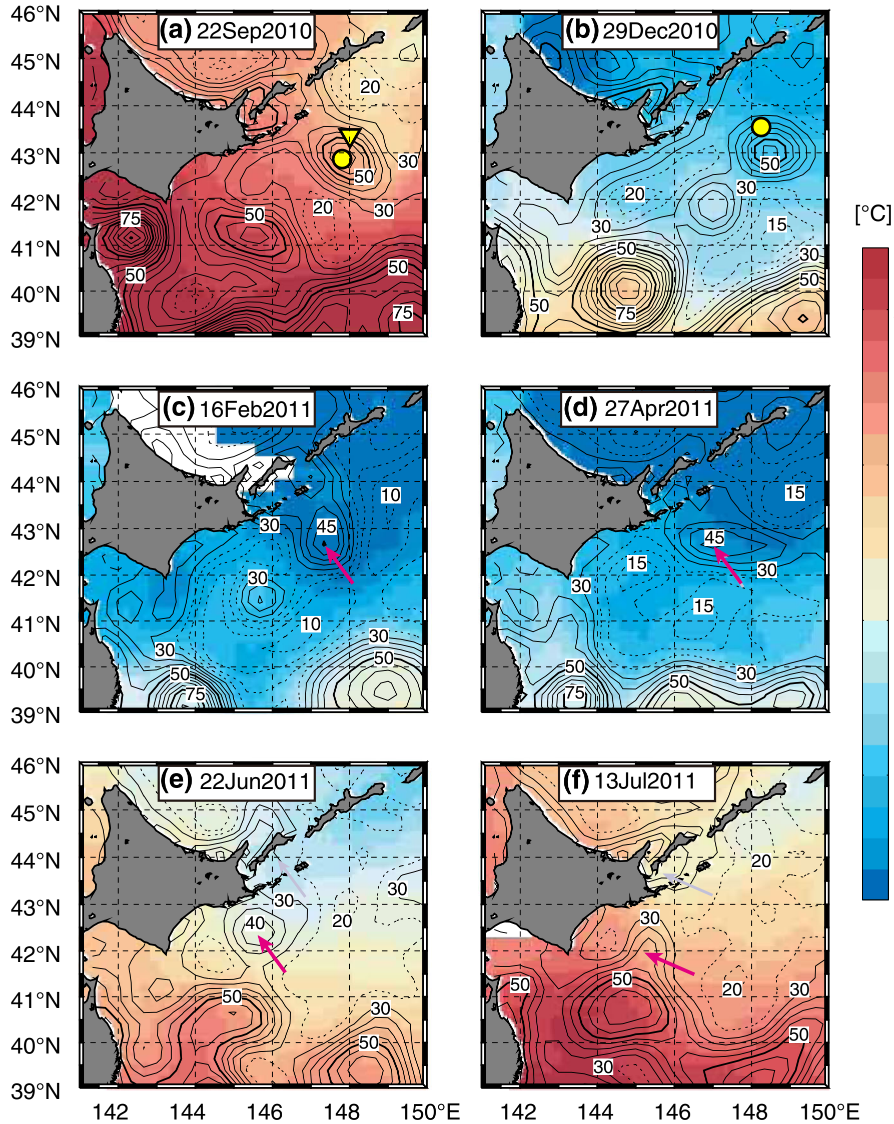

Fig. 11 As for Fig. 1, but for the period from September 2010 until July 2011 when Ring K09 was absorbed into a large intense warm-core ring. The positions of Ring K09 when no float data were available are estimated using SSH maps and are shown by *pink arrows*

relatively cold surface water (Fig. 11). In June 2011, Ring K09 was observed at 42°40′N, 145°32′E, and contacted the crest of a warm water meander (Fig. 11e). The crest was pinched off from the meander to become an intense warm-core ring, and Ring K09 was finally absorbed into this ring.

4 Discussion and conclusions

This study has demonstrated that Ring K09, initially observed as an anticyclonic ring with warm and saline core water, was modified by the intrusion of cold water (the cold-water event) from the southeastern coastal area off Hokkaido. As a consequence of this cold-water event, the warm core became significantly smaller and the cold water (typically <2.5 °C) arose within the ring below and adjacent to the warm core (lower and outer cores, respectively). Despite this drastic modification, Ring K09 remained an anticyclonic ring, as the lower and outer cores had low potential density and depressed the isopycnal surfaces downward.

Ring K09 was not a newly generated ring when it entrained float A in January 2009. Based on previous studies, the core water of 7–8 °C suggests that it had cooled from the 14–15 °C water of the Kuroshio Extension mainly through winter cooling (Tomosada 1986; Yasuda et al. 1992). Regeneration of these mature rings can be caused by the external supply of core water, but it was generally thought to be caused by warm water from the Kuroshio Extension or other warm-core rings (e.g., Yasuda et al. 1992). While previous observations of the co-existence of cold and warm waters within anticyclonic rings suggested the contribution of cold water (Yasuda et al. 2000; Itoh and Yasuda 2010b), the present study shows direct evidence of the regeneration of Kuroshio warm-core rings by the intrusion of cold water with low potential vorticity. If the surface water of the rings is substantially covered by cold water, as observed for Ring K09, they are less susceptible to winter cooling than typical warm-core rings. In addition, as cold water with low potential vorticity is occasionally supplied to the ring, as observed for Ring K09 (Fig. 3c), it is less likely that these cold rings simply spin down and decay within the subarctic gyre.

A more probable fate for the cold-core anticyclonic rings is that they propagate southwestward to be absorbed by the Kuroshio Extension or relatively new warm-core rings, as observed for Ring K09. Itoh and Yasuda (2010a) used satellite altimetry data to quantify the propagation of mesoscale eddies in the Kuroshio–Oyashio Extension region. Although they paid more attention to the northeastward propagation of anticyclonic eddies along the Japan and Kuril–Kamchatka Trench, the southwestward propagation along the coastal side of the trenches was also estimated (their fig. 8a). The poleward propagation of anticyclonic eddies were attributed to a pseudo-β effect caused by deep northeastward currents (Yasuda et al. 2000), or the image effect of the steep slope of the western boundary (Itoh and Sugimoto 2001). However, these mechanisms do not explain the turning of the propagation to the southwest. Interactions with the bottom topography, the other cold-core anticyclonic rings originating from the Sea of Okhotsk, and the synoptic-scale flow of the Oyashio current that is toward southwestward along the coast of Hokkaido, may also play a role in the above reversal, and this will be examined in future studies.

The direct cause of the cold-water event was the intrusion of the cold water into Ring K09 from the southeastern coastal area off Hokkaido. The potential temperature and potential vorticity of this cold water were <2 °C and $<15 \times 10^{-11}$ m^{-1}s^{-1}, respectively, which is consistent with the range of the water from the Sea of Okhotsk as suggested by Yasuda (1997). Therefore, we conclude that Ring K09, originating from the Kuroshio Extension, entrained the water originating from the Sea of Okhotsk. We further suggest that the strong tidal mixing in the Kuril Strait (Itoh and Yasuda 2010b; Itoh et al. 2011b, 2013; Yagi and Yasuda 2012) contributes to the formation of this cold and thick water mass.

We have shown the contributions of the cold water masses to renew the anticyclonic ring, but the inventory of the warm and cold waters has not been completed. This is mainly because the observations did not cover the whole area in and around Ring K09. Although the slight cooling of the upper core after the cold water event indicates the partial mixing of the warm and cold waters, it does not fully explain the drastic shrink of the upper core in its volume. It is suggested that some of the warm water extruded from the ring, whereas Float B did not leave the ring at that time. We assume that this was partly because the water exchange occurred partially within the ring, and partly because the parking depth of float B (500 dbar) was deeper than depths of the exchange.

The cold, fresh, and thick outflow from the Sea of Okhotsk is known for its substantial contribution to the North Pacific Intermediate Water, and is widely distributed within the subtropical North Pacific (Yasuda 1997). Intensive surveys of water properties and horizontal velocity to the east of Japan revealed that the coastal branch of the Oyashio current is one of the pathways from the Sea of Okhotsk to the subtropical gyre, while transport through isopycnal mixing has also been suggested, especially in offshore areas (Masujima et al. 2003; Yasuda 2004). The findings of the present study indicate that some of the water from the Sea of Okhotsk is transported with southwestward-propagating anticyclonic rings through the coastal path (after the reversal); if the anticyclonic ring with the cold and fresh water originating from the Sea of Okhotsk was absorbed into the Kuroshio Extension, the transport from the Sea of Okhotsk to the subtropical gyre would be completed. However, as the cold-water intrusion also occurs in the northeastward-propagating path before the reversal as Ring K09, the water properties would be modified when compared with the pathway in the Oyashio current. This is partly consistent with the findings of Talley et al. (1995), who suggested intrusions of the Oyashio water into warm-core rings and subsequent water mass modification.

Rings in the ocean have anomalous (either positive or negative) heat, kinetic energy, vorticity, and chemical constituents such as salt and nutrients. The transport and distribution of these properties are governed by the behavior and fate of the rings. In the northwestern North Pacific, anticyclonic rings transport subtropical water into the middle of the subarctic gyre, entrain the cold water from the Sea of Okhotsk, and then propagate towards the subtropical gyre. These processes enhance cross-gyre exchange and mixing of the above water properties in this region. Comprehensive exploration of the processes associated with ring propagation, and their interaction with other water masses, is anticipated in future studies, which will extend our understanding of the roles of intense mesoscale eddies in cross-gyre fluxes in the global ocean.

Acknowledgments The authors thank members of the Fisheries Environmental Oceanography group of the Atmosphere and Ocean Research Institute, The University of Tokyo, for their help in acquiring the profiling float data. The hydrographic data obtained by the R/V *Wakataka-Maru* were provided by the Tohoku National Fisheries Research Institute. This research was supported by the Ministry of Education, Science, Sports and Culture of Japan via a Grant-in-Aid for Scientific Research (KAKENHI) (S) 20221002, (B) 23310002, and Innovative Areas 24121002, and the Global Warming Project supported by the Ministry of Agriculture, Forestry and Fisheries Japan.

References

Brown OB, Cornillon PC, Emmerson SR, Carle HM (1986) Gulf-Stream warm rings—a statistical study of their behavior. Deep-Sea Res 33:1459–1473

Chelton DB, Schlax MG, Samelson RM, de Szoeke RA (2007) Global observations of large oceanic eddies. Geophys Res Lett 34. doi:10.1016/0198-0149(86)90062-2

Cresswell GR (1982) The coalescence of 2 east australian current warm-core eddies. Science 215:161–164. doi:10.1126/science.215.4529.161

Evans RH, Baker KS, Brown OB, Smith RC (1985) Chronology of warm-core ring 82b. J Geophys Res 90:8803–8811

Gordon AL (1985) Indian-Atlantic transfer of thermocline water at the agulhas retroflection. Science 227:1030–1033

Isern-Fontanet J, Garcia-Ladona E, Font J (2003) Identification of marine eddies from altimetric maps. J Atmos Ocean Tech 20:772–778

Itoh S, Sugimoto T (2001) Numerical experiments on the movement of a warm-core ring with the bottom slope of a western boundary. J Geophys Res 106:26851–26862

Itoh S, Yasuda I (2010a) Characteristics of mesoscale eddies in the Kuroshio-Oyashio extension region detected from the distribution of the sea surface height anomaly. J Phys Oceanogr 40:1018. doi:10.1175/2009jpo4265.1-1034

Itoh S, Yasuda I (2010b) Water mass structure of warm and cold anticyclonic eddies in the western boundary region of the subarctic North Pacific. J Phys Oceanogr 40:2624–2642. doi:10.1175/2010jpo4475.1

Itoh S, Shimizu Y, Ito S, Yasuda I (2011a) Evolution and decay of a warm-core ring within the western subarctic gyre of the North Pacific, as observed by profiling floats. J Oceanogr 67:281–293. doi:10.1007/S10872-011-0027-2

Itoh S, Yasuda I, Yagi M, Osafune S, Kaneko H, Nishioka J, Nakatsuka T, Volkov YN (2011b) Strong vertical mixing in the Urup Strait. Geophys Res Lett 38 Artn, L16607, doi: 10.1029/2011gl048507

Itoh S, Tanaka S. Osafune Y, Yasuda I, Yagi M, Kaneko H, Konda S, Nishioka T, Volkov YN (2013) Direct breaking of large-amplitude internal waves in the Urup Strait, Prog. Oceanogr, submitted

Joyce T, Backus R, Baker K, Blackwelder P, Brown O, Cowles T, Evans R, Fryxell G, Mountain D, Olson D, Schlitz R, Schmitt R, Smith P, Smith R, Wiebe P (1984) Rapid evolution of a Gulf-Stream warm-core ring. Nature 308:837–840

Kawai H (1972) Hydrography of the Kuroshio extension. In: Stommel H, Yoshida K (eds) Kuroshio, it's physical aspects. University of Tokyo Press, Tokyo, pp 235–352

Kitano K (1975) Some properties of warm eddies generated in confluence zone of Kuroshio and Oyashio currents. J Phys Oceanogr 5:245–252

Lutjeharms JRE (1988) Meridional heat-transport across the sub-tropical convergence by a warm eddy. Nature 331:251–254

Masujima M, Yasuda I, Hiroe Y, Watanabe T (2003) Transport of Oyashio water across the subarctic front into the mixed water region and formation of NPIW. J Oceanogr 59:855–869

Mizuno K, White WB (1983) Annual and interannual variability in the Kuroshio current system. J Phys Oceanogr 13:1847–1867

Okubo A (1970) Horizontal dispersion of floatable particles in vicinity of velocity singularities such as convergences. Deep-Sea Res 17:445–454

Olson DB, Fine RA, Gordon AL (1992) Convective modifications of water masses in the Agulhas. Deep-Sea Res 39:S163–S181

Richardson PL (1983) Gulf stream rings. In: Robinson AR (ed) Eddies in marine science. Springer, Berlin, pp 17–45

Sakaida F, Kawamura H, Takahashi S, Shimada T, Kawai Y, Hosoda K, Guan L (2009) Research and development of the New Generation Sea Surface Temperature for Open Ccean (NGSST-O) product and its demonstration operation. J Oceanogr 65:859–870. doi:10.1007/s10872-009-0071-3

Talley LD, Nagata Y, Fujimura M, Iwao T, Kono T, Inagake D, Hirai M, Okuda K (1995) North pacific intermediate water in the Kuroshio Oyashio mixed water region. J Phys Oceanogr 25:475–501

Tomosada A (1986) Generation and decay of Kuroshio warm-core rings. Deep-Sea Res 33:1475–1486

Weiss J (1991) The dynamics of entrophy transfer in two-dimensional hydrodynamics. Physica D 48:273–294

Yagi M, Yasuda I (2012) Deep intense vertical mixing in the Bussol' Strait. Geophys Res Lett. doi:10.1029/2011GL050349

Yasuda I (1997) The origin of the North Pacific intermediate water. J Geophys Res 102:893–909

Yasuda I (2003) Hydrographic structure and variability in the Kuroshio-Oyashio transition area. J Oceanogr 59:389–402

Yasuda I (2004) North Pacific intermediate water: progress in SAGE (SubArctic Gyre Experiment) and related projects. J Oceanogr 60:385–395

Yasuda I, Okuda K, Hirai M (1992) Evolution of a Kuroshio warm-core ring—variability of the hydrographic structure. Deep-Sea Res 39:S131–S161

Yasuda IY, Ito S, Shimizu Y, Ichikawa K, Ueda K, Honma T, Uchiyama M, Watanabe K, Sunou N, Tanaka K, Koizumi K (2000) Cold-core anticyclonic eddies south of the Bussol' Strait in the northwestern subarctic Pacific. J Phys Oceanogr 30:1137–1157